OH), 8.41 (s, 1H, ArH), 8.01 (dd, J=7.8, 1.0 Hz, 1H, ArH), 7.78 (t, J=8.3 Hz, 1H, ArH), 7.42 (d, J=8.8, 1.0 Hz, 1H, ArH), 5.06 (ddd, J=4.4, 3.0, 1.9 Hz, 1H, $C_{7eq}H$), 4.07 (s, 3H, OMe), 2.96 (s, 1H, C_7OH), 2.53 (dd, J=14.7, 3.0 Hz, 1H, $C_{8eq}H$), 2.24 (dd, J=14.7, 4.4 Hz, 1H, $C_{8ax}H$), 1.81-1.76 (m, 2H, $C_{13}H$), 0.92 (t, J=7.1 Hz, 3H, $C_{14}H$); ^{13}C NMR ($CDCl_3$) δ 199.91, 188.70, 180.40, 160.65, 160.42, 136.01, 135.56, 134.21, 133.03, 132.88, 121.79, 119.79, 118.92, 118.02, 117.84, 70.55, 63.52, 56.69, 40.18, 7.29; MS (m/z), 282 (M^+).

20b: ^1H NMR ($CDCl_3$) δ 13.36 (s, 1H, OH), 8.38 (s, 1H, ArH), 8.00 (dd, J=7.8, 1.0 Hz, 1H, ArH), 7.80 (t, J=8.0 Hz, 1H, ArH), 7.43 (dd, J=8.1, 1.0 Hz, 1H, ArH), 5.37 (ddd, J= 9.3, 6.1, 3.4 Hz, 1H, $C_{7ax}H$), 4.07 (s, 3H, OMe), 3.66 (d, J= 3.4 Hz, 1H, C_7OH), 2.79 (dd, J=13.7, 6.1 Hz, 1H, $C_{8eq}H$), 2.24 (dd, J=13.7, 9.3 Hz, 1H, $C_{8ax}H$), 1.76-1.56 (m, 2H, $C_{13}H$), 0.92 (t, J=7.3, Hz, 3H, $C_{14}H$); ^{13}C NMR ($CDCl_3$) δ 199.45, 189.17, 180.15, 160.81, 160.31, 137.47, 135.51, 135.19, 134.84, 132.56, 121.37, 119.70, 119.47, 119.35, 117.89, 76.19, 63.63, 40.28, 29.82, 7.24; MS (m/z) 282 (M^+).

Acknowledgment. This work was supported by the Basic Science Research Institute Program of Ministry of Education (to YSR, BSRI-97-3431) and by the Korea Basic Science Institute (to CC).

References

1. Krassilnikov, N. A.; Koreniakov, A. *J. Mikrobiologiya (USSR).* **1939**, *8*, 673.
2. Brockmann, H.; Frank, B. *Chem. Ber.* **1955**, *88*, 1792.
3. Arcamone, F. *Doxorubicin Anticancer Antibiotics*, Academic Press: New York, U.S.A. 1981; Vol. 17, pp 319-329.
4. Priebe, W. *Anthracycline Antibiotics*, ACS Symposium Series 574, 1995.
5. Tone, H. *Drugs Exptl. Clic. Res.* **1985**, *XI*(1), 9.
6. Arcamone, F.; Cassinelli, G.; DiMatteo, F.; Forenza, S.; Ripamonte, M. C.; Rivola, G.; Vigenvani, A.; Clardy, J.; McCabe, T. *J. Am. Chem. Soc.* **1980**, *102*, 1462.
7. Rho, Y. S.; Park, S. H.; Kim, S. Y.; Cho, I. H.; Lee, C. H.; Kang, H. S.; Cheong, C. J. *Bull. Kor. Chem. Soc.* **1998**, *19*(1), 74.
8. (a) Hauser, F. M.; Hewawasam, P.; Rho, Y. S. *J. Org. Chem.* **1989**, *54*, 5110. (b) Rho, Y. S.; Yoo, J. H.; Baek, B. N.; Kim, C. J.; Cho, I. H. *Bull, Kor. Chem. Soc.* **1996**, *17*, 946. (c) Rho, Y. S.; Kim, S. J.; Cho, I. H. *J. Pharm. Soc. Kor.* **1997**, *41*, 7. (d) Rho, Y. S.; Park, S. H.; Kwon, Y. J.; Kang, H. S.; Cho, I. H. *J. Kor. Chem. Soc.* **1995**, *39*, 218.
9. Schlosser, M.; Christmann, K. F. *Justus Liebigs, Ann. Chem.* **1967**, *708*, 1.
10. Boeckman, Jr. R. K.; Sum, F.-W. *J. Am. Chem. Soc.* **1982**, *104*, 4604.
11. Giolitti, A.; Guidi, A.; Pasqui, F.; Pestellini, V.; Arcamone, F. *Tetrahedron Lett.* **1992**, *33*, 1637.
12. Coburn, C. E.; Anderson, D. K.; Swenton, J. S. *J. Org. Chem.* **1983**, *48*, 1455.
13. Tanaka, H.; Yoshioka, T.; Shimauchi, Y.; Yoshimoto, A.; Ishikura, T. *Tetrahedron Lett.* **1984**, *25*, 3355.
14. Kita, A.; Maeda, H.; Kirihara, M.; Fujii, Y.; Nakajima, T.; Yamamoto, H.; Tamura, Y.; Fujioka, H. *Chem. Pharm. Bull.* **1992**, *40*, 61.
15. Keay, B. A.; Rodrigo, R. *Tetrahedron* **1984**, *40*, 4597.

Rapid Energy Transfer Mechanism of F Electronic Excitation to the Vibration of Randomly Distributed OH^- in KCl

Du-Jeon Jang* and Chil Seong Ah

Department of Chemistry and Research Institute of Molecular Sciences, Seoul National University, Seoul 151-742, Korea
Received June 13, 1998

The nature of F electronic excitation energy transfer to OH^- vibrational levels in KCl crystals is the exchange interaction, although the transfer process exhibits three temporally distinguishable components depending on the distance between excited F center and OH^-. The critical distance as well as rate of the major energy transfer process in randomly distributed samples increases rapidly as OH librational motions become active with temperature rise. The excited state character introduced into the OH^- ground electronic state by perturbation is essential for the exchange interaction. The perturbation is brought about by the expanded electron cloud of excited F center for OH^- associated to F center, whereas by librations and lattice vibrations perpendicular to the bond axis for isolated OH^-. F excitation quenching efficiency by OH^- is dependent on the variation of the critical distance rather than the rate as the rate is much faster than the normal F bleach recovery rate.

Introduction

This is the final paper concluding a series of studies[1-4] on the bleach recovery kinetics of F centers in alkali halides. F absorption bleach in OH^- doped crystals recovers with four temporally distinguishable components designated as super-

fast, fast, medium, and slow processes.[1-3] The early three ones are consequent on rapid energy transfer from electronically excited F centers to OH^- vibrational levels while the slow one is due to the normal relaxation process of electronically excited, lattice-vibrationally relaxed F (F^*) centers as found in OH^- free crystals. The superfast is the major relaxation channel in optically aggregated samples and resulting from the energy transfer between the associated pair of F^* and OH^-,[1,3] while the medium is the major quenching process in randomly distributed crystals and due to interaction between relatively widely separated F^* and OH^- defects.[2] However, the fast one is a minor process in any kinds of samples and it is accounted by the relaxation of the F^* center which is partially associated to OH^- defect.[2] Although the quenching processes of F excitation by OH^- defects have been investigated phenomenologically, the nature of the electronic coupling between F^* and OH^- defects has not been examined yet. The main purposes of this paper are to show the nature of the energy transfer from the F^* electronic state to OH^- vibrational states and to explain the reported quenching efficiency behaviors of F excitation by OH^- defects.

Quantum mechanically there are two types of electronic interactions for the electronic excitation energy transfer from an excited donor species (D*) to a ground state acceptor species (A), namely, H_e, the exchange interaction and H_c, the Coulombic interaction, by which $\Psi(D^*)\Psi(A)$ can undergo transition to $\Psi(D)\Psi(A^*)$.[5] Thus we can relate the probability of electronic interaction to an experimental quantity, the rate constant of energy transfer k_{ET},

$$k_{ET} \sim [<\Psi(D)\Psi(A^*) \mid H_e \mid \Psi(D^*)\Psi(A)>^2 + <\Psi(D)\Psi(A^*) \mid H_c \mid \Psi(D^*)\Psi(A)>^2] \quad (1)$$

to understand the nature of the electronic coupling. Depending on the matrix elements of the Coulombic interaction Hamiltonian, there are dipole-dipole, dipole-quadrupole, quadrupole-quadrupole, ..., interactions. However, since only the dipole-dipole interaction among the Coulombic interactions is necessary to consider for the energy transfer between F^* and OH^- defects, we compare our experiential results with the theoretical equations derived for the exchange and dipole-dipole interactions only.

The F^* centers in rubidium and potassium halides emit a highly efficient and long-lived luminescence at cryogenic temperature, whereas those in lithium and sodium halides have a poor luminescence.[6,7] This remarkable difference in two types of hosts is explained by the difference in crossover energy barriers from the lattice-vibrationally relaxed, excited electronic potential well to the crossing point of the excited and ground state potential curves.[8-10] However, the luminescence in KCl, in which the barrier is too high for effective crossover, is reported[11,12] to decrease drastically with the concentration increment of doped molecular defects such as OH^- and CN^-. Vibrational emission and anti-Stokes Raman scattering from molecular defects observed after F excitation indicate that the electronic excitation energy transfers into the stretching vibrational mode of a molecular defect.[13-15] Researches on the interactions of F centers with OH^- [16-18] and CN^- [19,20] and on related topics to these interactions[21-24] have been extensively carried out. Our previous results of energy transfer kinetic studies by monitoring F bleach recovery profiles are introduced briefly in the beginning of this paper.

Experimental

Experimental procedures, shown in detail already,[2] are briefed here. The typical mole fraction of additively introduced F center is 5×10^{-5} and this is at least two orders of magnitude lower than OH^- concentrations. In order to produce samples with isolated and randomly distributed F centers, crystals were heated to 750 K, cooled to room temperature immediately, mounted on a cold finger, and then cooled to cryogenic temperature without light exposure. F band light illumination to these samples at 240 K migrates F centers toward OH^- defects, finally forming associated pairs, $F_H(OH^-)$ centers. If not mentioned as aggregated, defects in our samples are randomly distributed.

The principles of the picosecond transient absorption spectrometer utilizing dye emission and a streak camera employed to measure F absorption bleach recovery profiles were previously[25] described in detail. Fluorescence from laser dye, excited by the pulses from a mode-locked Quantel 471 Nd:YAG laser, was used to probe the transient absorption of sample generated by 532-nm laser pulses. A Hamamatsu C979 streak camera with a 10-ps time resolution, coupled to a Princeton Applied Research intensified 1420 Reticon, was used as the detector. The comparison of dye emission kinetic profiles measured by the streak camera without and with sample excitation yields a picosecond bleach recovery kinetic profile. Bleach recovery times were extracted by fitting measured kinetic profiles to computer simulated recovery curves convoluted with the instrument response function.

Results and Discussion

The typical bleach recovery profiles in Figure 1 of randomly distributed, OH^- doped KCl crystal show that the relative amplitude as well as rate of the medium process increases and decreases reversibly with temperature incline

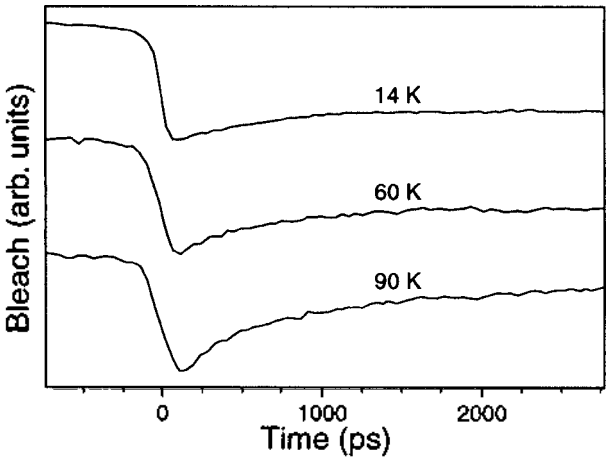

Figure 1. F absorption bleach recovery profiles of F centers in OH^- (2.3×10^{-3} in mole fraction) doped KCl measured at three different temperatures, showing that the relative amplitude, plus rate, of the medium process enlarges with temperature increment.

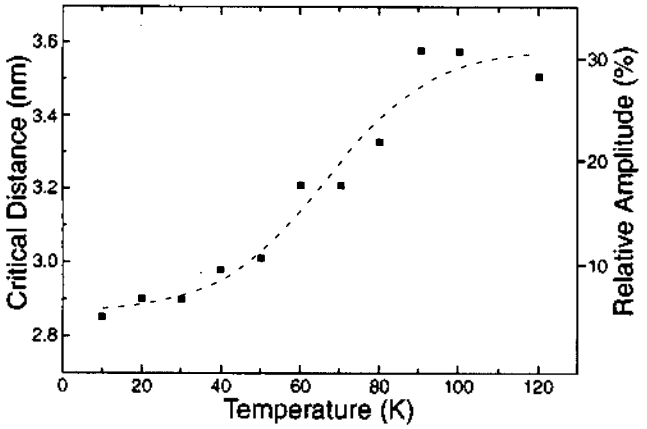

Figure 2. Relative amplitude (square) and fitted critical distance (dotted curve) changes of the medium process with temperature variation for the same sample as in Figure 1.

and decline, respectively. The temperature-dependent variation of the relative amplitude of the medium component is very similar to the temperature behaviors of medium relaxation rate[2] and F luminescence quenching efficiency ($1-\eta_F$) by OH^-.[26] Knowing the concentration of randomly distributed OH^- and the relaxation time of the medium process which is negligibly shorter than that of the normal slow process, we can calculate the critical distance of the medium energy transfer process as the dotted curve in Figure 2. Since the lattice parameter (**a**) of KCl is 6.29 Å,[27] the critical distance is about 4.5 **a** below 90 **K** and becomes 5.5 **a** above 90 K. The relative percent amplitudes of the superfast and fast relaxation processes do not change with temperature variation and these also can be converted into the critical distances as well. In such a way we have noticed that the relative percent amplitudes of the superfast and fast components are significantly higher than those expected in so-called randomly distributed samples, suggesting that **F** centers are not completely isolated and randomly distributed.

Taking account of the results from optically aggregated samples and literaturely available facts about association between F and OH^- defects, the major relaxation processes of F excitation are schematically shown as a function of the distance between F* and OH^- in Figure 3. If an F center has an OH^- defect at one lattice parameter, **F** absorption spectrum from the ground state is broadened by associating with OH^- and excitation energy transfers within a few picoseconds *via* the superfast process.[1,3] If an F center has at least one OH^- within two and half lattice parameters outside the superfast process range, even though F absorption is not affected by OH^-, excitation energy transfers rapidly through the fast process. The fast transfer is possible *via* overlap caused by the widely extended orbital of the F* center. The electron cloud spreaded already in the ground state of the F center is reported[28] to expand further to the peak radius of 6.84 Å in the excited state. The medium process occurs if an F center has at least one OH^- defect within about five lattice parameters, although the critical interaction distance increases with temperature rise. We need to examine more carefully how the electronic interaction between F* and OH^- defects at

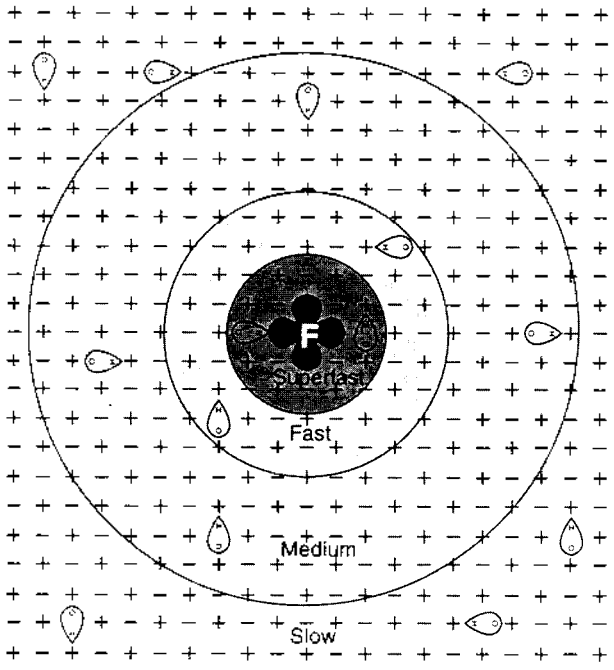

Figure 3. Schematic representation of OH^- distance-dependent major relaxation processes of F excitation energy in KCl.

the distance of 5 **a** occurs so rapidly for the medium energy transfer process.

Figure 4 shows the Arrhenius plots of the medium

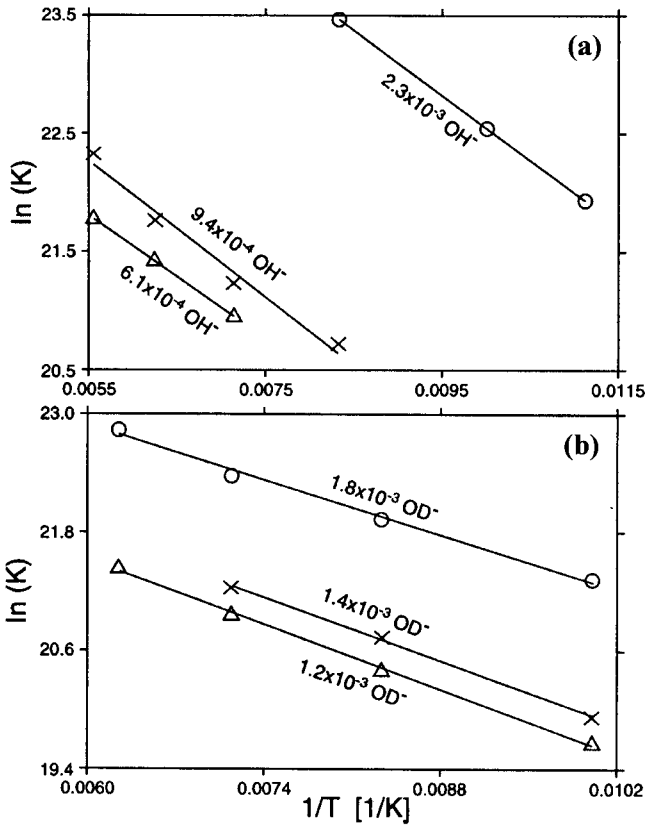

Figure 4. Arrhenius plots of the medium relaxation rates for OH^- (a) and OD^- (b) doped samples. The OH^-/OD^- concentrations in mole fraction are indicated near the respective plots.

relaxation rates measured above 90 K. The activation energies are 380, 400, and 360 cm^{-1} for 2.3×10^{-3}, 9.4×10^{-4}, and 6.1×10^{-4} OH doped samples (a), respectively, and 280, 320, and 320 cm^{-1} for 1.8×10^{-3}, 1.4×10^{-3}, and 1.2×10^{-3} OD^- doped samples (b), respectively. The average activation energies are 380 and 310 cm^{-1} for OH^- and OD^- doped samples respectively and these are related to the librational energies of OH^- and OD^- in KCl respectively.[29] The librational energy of OH^- in KCl is reported to be 300-400 cm^{-1} and that of OD^- is reduced by a factor of ~1.3.[29,30] Below 90 K the medium relaxation rate increases linearly with temperature. So the medium process is assisted predominantly by one phonon processes[31] below 90 K while by librational motions above 90 K.

In order to understand the nature of the electronic coupling, the temporal behaviors of typical bleach recovery profiles are compared with the theoretical linear equations of the dipole-dipole and exchange interactions in Figure 5. Since the instrument has a finite response time, the starting bleach recovery time is set to the half maximum rise and only the datum points after the bleach maxima are used to fit. For the three-dimensional dipole-dipole interaction, the average donor population P_d is derived[32,33] to reduce with time t as

$$P_d \sim \exp(-t/\tau_0)\exp(-(t/\tau)^{1/2}), \quad (2)$$

where τ_0 and τ are the lifetime of D* observed in absence and presence, respectively, of A. Eq. (2) can be simplified as

$$P_d \sim \exp(-(ln(t/\tau)^{1/2})), \quad (3)$$

for τ_0 is much larger than τ in our samples. If the bleach is recovered in consequence of energy transfer and if the nature of the energy transfer is the dipole-dipole interaction, the plots of ln(Bleach) *vs* $(t)^{1/2}$ should be linear. Nevertheless, the plots in Figure 5(a) are significantly curved in the early time scale, especially at the highest OH- concentration.

Now we consider energy transfer via the resonance electronic exchange mechanism, assuming that no back transfer from A* to D is allowed. It is verified[34,35] that when the experimental measurement is carried out at the time much longer than the transfer time between the nearest neighbors, the donor population can be written simply as

$$P_d \sim \exp(-c(ln(t/\tau_n)^L)), \quad (4)$$

where L is the Euclidian dimension, τ_n is energy transfer time to the nearest neighbor, and c is a constant. Considered the temperature dependence of superfast transfer rate[1,3,4] and the <200> arrangement of $F(OH^-)$ center,[18] τ_n has been estimated to be ~0.1 ps at 120 K and L is 3 for the current system. All the plots in Figure 5(b) show good linearities, suggesting that the nature of the energy transfer process is the exchange interaction.

Despite the fact that Figure 5 indicates the exchange interaction as the nature of the energy transfer, there are two facts, the fully filled electronic configuration of OH^- and the large critical interaction distance of the medium process, that are usually not appropriate for the exchange interaction. Considering that atomic orbitals of $(1s)_H$ and $(2p)_O$ only, we can write the ground and lowest excited electronic configurations of OH^- simply as $(\sigma)^2(n_{xy})^4$ and $(\sigma)^2(n_{xy})^3(\sigma^*)^1$ respectively. The additional electron cloud supplied by the widely extended orbital of the associated F* perturbs the ground configuration of OH^- to make $(\sigma)^2(n_{xy})^4+\delta(\sigma)^2(n_{xy})^3(\sigma^*)^1$ for the superfast and fast processes. For the medium process, in which the critical distance is about 5 **a**, neither any overlap between F* and OH^- electronic wavefunctions nor any partially filled orbital character at the OH^- ground configuration seems to exist at a glance. Since, as mentioned before, wavefunctional overlap between D* and A and unfilled orbitals for both D* and A are prerequisite to the exchange interaction, we have to see if these requisites can be fulfilled by other phenomena we can observe. We have seen from the temperature dependence that the medium process is assisted predominantly by librational motions above 90 K while by one phonon processes below 90 K. It is quite interesting to note that from a simple symmetry consideration

$$<(\sigma)^2(n_{xy})^3(\sigma^*)^1 \mid (R_x, R_y) \mid (\sigma)^2(n_{xy})^4> \neq 0 \quad (5)$$

$$<(\sigma)^2(n_{xy})^3(\sigma^*)^1 \mid R_Z \mid (\sigma)^2(n_{xy})^4> = 0. \quad (6)$$

These suggest that motions perpendicular to OH^- bond axis

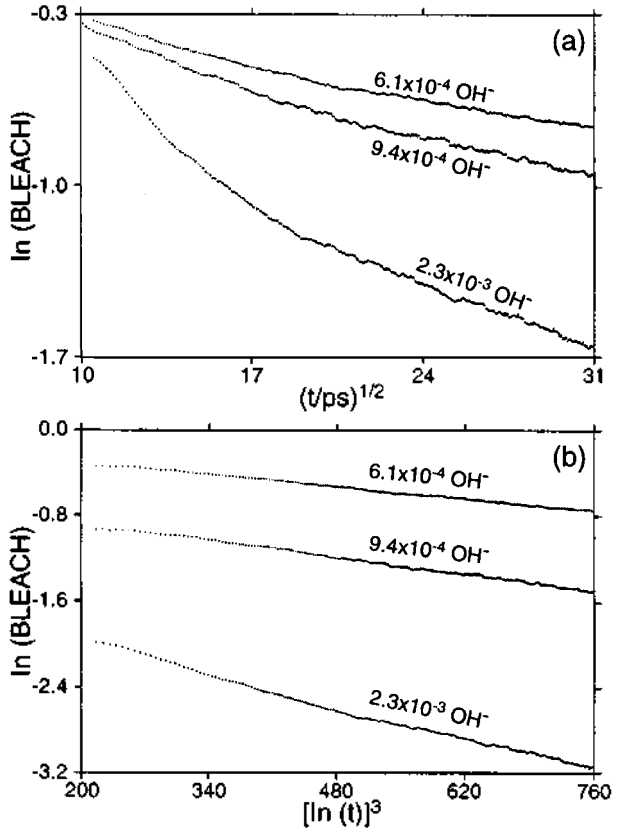

Figure 5. Bleach recovery temporal profiles, measured at 120 K for the same samples as in Figure 4(a), plotted according to the linear equations of theoretical dipole-dipole interaction (a) and exchange interaction (b) mechanisms. Only the bleach recovery datum points after the bleach maxima of the profiles are plotted and the starting recovery time was set to the half maximum rise of the bleach. The energy transfer time to the nearest neighbor was set to 0.1 ps for the exchange mechanism.

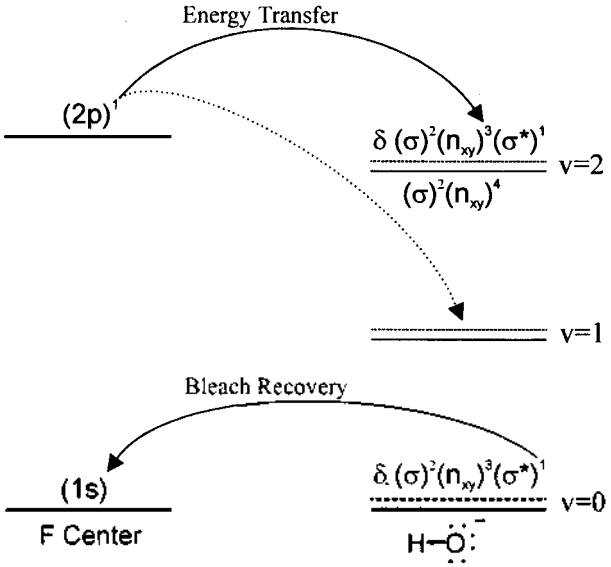

Figure 6. Schematic representation of energy transfer mechanism of F electronic excitation to the vibrational levels of randomly distributed OH⁻ in KCl, showing that the exchange resonance interaction of $<\Psi(D)\Psi(A^*) \mid H_e \mid \Psi(D^*)\Psi(A)>$ ends in OH^- vibrational excitation and F excitation quenching.

such as liberational motions and a certain lattice vibrations may introduce the excited state character into the ground state of OH^-. The enlargement of, not only the rate but also, the critical distance with the activation of librational motions as well as some types of lattice vibrations supports this perturbation to be plausible so that the ground state configuration of OH^- can be written as $(\sigma)^2(n_{xy})^4+\delta(\sigma)^2(n_{xy})^3(\sigma^*)^1$ for the medium process along with those shown before for the superfast and fast processes. Since the excited state of $(\sigma)^2(n_{xy})^3(\sigma^*)^1$ is reported[36] to possess a large 3s-Rydberg state character, the perturbed electronic wavefunction has some delocalized character so that it can overlap with the largely expanded wavefunction of F* center.

Admitting that three different energy transfer processes are temporally distinguishable depending on the distance between F* and OH^- defects and that the perturbation methods introducing the excited state character into the ground electronic state are different among three transfer processes, the electronic configuration of OH^- involved in three energy transfer processes is $(\sigma)^2(n_{xy})^4+\delta(\sigma)^2(n_{xy})^3(\sigma^*)^1$. This perturbed configuration has unfilled, even if very small, orbital character, which is indispensable to the resonance exchange interaction, and its wavefunction is, in the above, suggested to overlap with the 2p orbital electron cloud of the donor F* center. The exchange interaction matrix of $<\Psi(D)\Psi(A^*) \mid H_e \mid \Psi(D^*)\Psi(A)>$ can be expressed briefly as

$$<(1s)_F[(n_{xy})^4\ \varphi_{vib}(f)]_{OH^-} \mid H_e \mid (2p)_F [(n_{xy})^3(\sigma^*)\ \varphi_{vib}(i)]_{OH^-}>, \quad (7)$$

where $\varphi_{vib}(f)$ and $\varphi_{vib}(i)$ are the final and initial vibrational wavefunctions of OH^-, respectively, and H_e could be $\sum_{Q_a(i>j)} \frac{\partial}{\partial Q_a}(\frac{e^2}{r_{ij}})$ from the first order perturbation theory. This matrix mainly represents a repulsion between two charge densities of $(1s)_F(n_{xy})_{OH^-}$ and $(2p)_F(\sigma^*)_{OH^-}$ and this does not vanish in view of a simple symmetry consideration. Figure 6 schematically represents the electronic exchange interaction involved in the energy transfer processes of F electronic excitation to OH^- vibrational levels. The electrostatic repulsion between the charge densities of $(1s)_F(n_{xy})_{OH^-}$ and $(2p)_F(\sigma^*)_{OH^-}$ wavefunctions results in the vibrational excitation of OH^- and the electronic relaxation of F* center. This electronic interaction can be conceptually visualized as the electron exchange in Figure 6. The (2p) electron of F center shifts into the perturbed (n_{xy}) orbital of OH^- at the same time that the electron introduced into the (σ^*) orbital of OH^- by perturbation shifts into the (1s) orbital of F center. As the results of this electronic exchange interaction, the repulsion between charge densities diminishes, F absorption bleach recovers, the electronically excited character of OH^- brought in by perturbation relaxes, and the vibrational quantum number of OH^- stretching mode enlarges by one or two.[14,15]

Conclusions

Some important results are obtained by putting together a series of studies on F electronic excitation energy transfer to OH^- vibrations in KCl. For all three temporally distinguishable components, the nature of the energy transfer is the exchange interaction rather than the Coulombic interaction such as the dipole-dipole interaction. The exchange interaction of F* center becomes effective with the small character of the lowest excited configuration $(\sigma)^2(n_{xy})^3(\sigma^*)^1$, which is perturbatively introduced by pairing with F center for the superfast component, by being overlayed with the expanded electron cloud of excited F center for the fast one, and by OH^- librations and/or lattice vibrations perpendicular to OH^- bond axis for the medium one. The temperature dependence of F luminescence quenching by OH^- is determined mainly by the variation of the critical distance rather than rate of the medium process with temperature change since the transfer rate is at least two orders of magnitude faster the normal F* relaxation rate. The critical transfer distance as well as rate of the medium process increases with temperature rise as the OH^- ground configuration is perturbed effectively by OH^- librational motions and lattice vibrations.

Acknowledgment. This work was supported by the S. N.U. Research Fund. DJ also acknowledges the Hallym Academy of Sciences, Hallym University and the Korea Ministry of Education.

References

†. Also a member of the Center for Molecular Science, Taejon 305-701, Korea.
1. Lee, S. Y.; Jang, D.-J. *Bull. Korean Chem. Soc.* **1997**, *18*, 121.
2. Jang, D.-J.; Kim, P. S. *Bull. Korean Chem. Soc.* **1995**, *16*, 1184.
3. Jang, D.-J.; Lee, J. *Solid State Commun.* **1995**, *94*, 539.
4. Chung, Y. B.; Lee, I. W.; Jang, D.-J. *Opt. Commun.* **1991**, *86*, 41.

5. Turro, N. J. *Modern Molecular Photochemistry*; Benjamin/Cummings: Menbo Park, California, U.S.A., 1978; p 300.
6. Markham, J. J. *F-Centers in Alkali Halides*; Academic Press: New York, U.S.A., 1966; p 1.
7. Bosi, L.; Bussolati, C.; Spinolo, G. *Phys. Rev. B* **1970**, *1*, 890.
8. Dexter, D. L.; Klick, C. C.; Russell, G. A. *Phys. Rev.* **1955**, *100*, 603.
9. Gomes, L.; Morato, S. P. *J. Appl. Phys.* **1989**, *66*, 2754.
10. De Matteis, F.; Leblans, M.; Slootmans, W.; Schoemaker, D. *Phys. Rev. B* **1994**, 13186.
11. Gomes, L.; Luty, F. *Phys. Rev. B* **1984**, *30*, 7194.
12. Casalboni, M.; Prosposito, P.; Grassano, U. M. *Solid State Commun.* **1993**, *87*, 305.
13. Yang, Y.; von der Osten, W.; Luty, F. *Phys. Rev. B* **1985**, *32*, 2724.
14. Halama, G.; Tsen, K. T.; Lin, S. H.; Luty, F.; Page, J. B. *Phys. Rev. B* **1989**, *39*, 13457.
15. Halama, G.; Tsen, K. T.; Lin, S. H.; Page, J. B. *Phys. Rev. B* **1991**, *44*, 2040.
16. Gustin, E.; Leblans, M.; Bouven, A.; Schoemaker, D. *Phys. Rev. B* **1996**, *54*, 6977.
17. Gustin, E.; Leblans, M.; Bouven, A.; Schoemaker, D. *Phys. Rev. B* **1996**, *54*, 6963.
18. Dierolf, V.; Luty, F. *Phys. Rev. B* **1996**, *54*, 6952.
19. Samiec, D.; Stolz, H.; von der Osten, W. *Phys. Rev. B* **1996**, *54*, 6977.
20. West, J.; Tsen, K. T. *Phys. Rev. B* **1994**, *50*, 9759.
21. Afanasiev, A.; Luty, F. *Solid State Commun.* **1996**, *98*, 531.
22. Lin, B. *Opt. Commun.* **1996**, *124*, 400.
23. Salminen, O.; Riihola, P.; Ozols, A.; Viitala, T. *Phys. Rev. B* **1996**, *53*, 6129.
24. An, C. P.; Luty, F. *Phys. Rev. B* **1997**, *56*, R5721.
25. Jang, D.-J.; Kelley, D. F. *Rev. Sci. Instrum.* **1985**, *56*, 2205.
26. Gomes, L.; Luty, F. *Phys. Rev. B* **1995**, *52*, 7094.
27. Kittel, C. *Introduction to Solid State Physics*; John Wiley & Sons: New York, U.S.A., 1976; p 21.
28. Mollenauer, L. F.; Baldacchini, G. *Phys. Rev. Lett.* **1972**, *29*, 465.
29. Klein, M. V.; Wedding, B.; Levine, M. A. *Phys. Rev. B* **1969**, *180*, 902.
30. Kapphan, S.; Luty, F. *Solid State Commun.* **1970**, *8*, 349.
31. Holstein, T.; Lyo, S. K.; Orbach, R. *Phys. Rev. B* **1977**, *6*, 934.
32. Inokuti, M.; Hirayama, F. *J. Chem. Phys.* **1965**, *43*, 1978.
33. Dexter, D. L. *J. Chem. Phys.* **1953**, *21*, 836.
34. Klafter, J.; Blumen, A. *J. Lumin.* **1985**, *34*, 77.
35. Yang, C.-L.; El-Sayed, M. A. *J. Phys. Chem.* **1986**, *90*, 5720.
36. Mario, H. J.; McGlynn, S. P. *J. Chem. Phys.* **1970**, *52*, 3402.

Molecular Dynamics Simulation Study on Segmental Motion in Liquid Normal Butane

Song Hi Lee* and Han Soo Kim†

Department of Chemistry, Kyungsung University, Pusan 608-736, Korea
†Department of Industrial Chemistry, Kangnung National University, Kangnung 212-702, Korea
Received June 13, 1998

We present results of molecular dynamic (MD) simulations for the segmental motion of liquid *n*-butane as the base case for a consistent study for conformational transition from one rotational isomeric state to another in long chains of liquid *n*-alkanes. The behavior of the hazard plots for *n*-butane obtained from our MD simulations are compared with that for *n*-butane of Brownian dynamics study. The MD results for the conformational transition of *n*-butane by a Poisson process form the total first passage times are different from those from the separate $t \rightarrow g$ and $g \rightarrow t$ first passage times. This poor agreement is probably due to the failure of the detailed balance between the fractions of *trans* and *gauche*. The enhancement of the transitions $t \rightarrow g$ and $g \rightarrow t$ at short time regions are also discussed.

Introduction

In recent papers,[1-3] we carried out equilibrium molecular dynamics simulations of three different models for liquid alkanes to investigate the thermodynamic, structural, and dynamic properties of liquid normal alkanes (*n*-butane to *n*-heptadecane) and branched alkanes (isobutane, 4-propyl heptane, 6-pentyl duodecane, and 5-dibutyl nonane). In the present paper the same technique is applied to study the segmental motion of normal butane as the base case for a consistent study of conformational transitions from one rotational isomeric state to another in long chains of liquid *n*-alkanes.

In recent years, there has been considerable experimental and theoretical interest in the dynamics of molecular conformational motion in solution. Computer simulation of